Transactions of the Materials Research Society of Japan 30[1] 23-26 (2005)

Ferroelectric Properties of $Ba_2NaNb_5O_{15}$ Thin Films Prepared by Pulsed Laser Deposition

Tohru Higuchi, Naoaki Machida, Taro Yamasaki, Takayuki Kamei,
Takeshi Hattori and Takeyo Tsukamoto
Department of Applied Physics, Tokyo University of Science, 1-3 Kagurazaka, Shinjuku, Tokyo 162-8601, Japan
Fax: 81-3-3260-4772, e-mail: higuchi@rs.kagu.tus.ac.jp

The *c*-axis-oriented $Ba_2NaNb_5O_{15}$ (BNN) thin films were prepared on $La_{0.05}Sr_{0.95}TiO_3$ substrates by pulsed laser deposition. The *c*-axis orientation and surface roughness of the BNN thin films depend on substrate temperature (T_{sub}) and oxygen gas pressure (Po_2) during the deposition. When T_{sub} and Po_2 were fixed at 700°C and 7.5 mTorr, respectively, the BNN thin film exhibited a strong *c*-axis orientation and a smooth surface. Its remanent polarization (P_r) and coercive field (E_c) were $2P_r$=48.5 μC/cm^2 and $2E_c$=290 kV/cm, respectively. The energy gap was approximately 3.1 eV, which accords with the BNN single crystal.

Key words: $Ba_2NaNb_5O_{15}$, Thin Films, Pulsed Laser Deposition, Band Gap, Remanent Polarization,

1. INTRODUCTION

$Ba_2NaNb_5O_{15}$ (BNN), which belongs to the point group of mm2 at room temperature, is ferroelectric oxide with a tetragonal tungsten bronze-type structure [1-6], as shown in Fig. 1. The BNN crystal has been expected as optical device because the nonlinear optical coefficient is twice as large as that of $LiNbO_3$ and 20 times higher than that of KH_2PO_4 [7,8]. In term of ferroelectricity, the BNN has two phase transitions above room temperature. One is ferroelectric phase transition at approximately 560°C, the other is ferroelastic phase transition at approximately 300°C, which is responsible for the formation of twined substructure. The BNN crystal has the spontanesous polarization of 40 μC/cm^2 and dielectric constant (ε) of 51 parallel to *c*-axis. However, in thin film form, it is difficult to confirm the ferroelectric and structural properties, which correspond to bulk crystal.

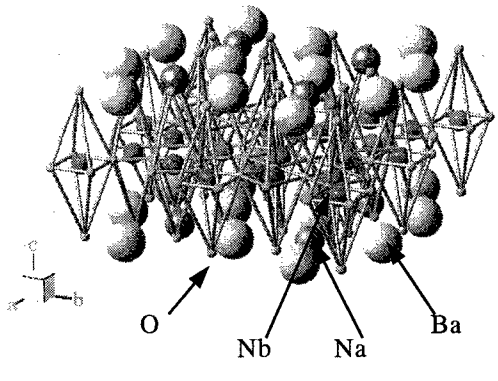

Fig. 1 Crystal structure of $Ba_2NaNb_5O_{15}$ (BNN).

In recent years, our groups have prepared the BNN thin films on La-doped $SrTiO_3$ ($La_{0.05}Sr_{0.95}TiO_3$: LSTO) substrates by pulsed laser deposition (PLD) method [12-16]. When the oxygen gas pressure and substrate temperature were fixed at 7.5 mTorr and 700°C, respectively, the BNN thin film exhibited a relatively good *P-E* hysteresis loop. Then, the remanent polarization (P_r) and coercive field (E_c) were $2P_r$=95.3 μC/cm^2 and $2E_c$=400 kV/cm [14], respectively, although the effect of leakage current was very large. To further investigate the ferroelectricity of BNN thin films prepared by PLD method, it is necessary to perform more systematic optimizations such as oxygen gas pressure (Po_2) and substrate temperature (T_{sub}) during the deposition.

In this study, the *c*-axis oriented BNN thin films were prepared on LSTO substrates by PLD method. It is known that the LSTO has a metallic conductivity at room temperature [17]. The lattice mismatch between BNN and LSTO was estimated to be approximately 5.2 % [14]. We report in this paper that the delicate control between T_{sub} and Po_2 during the deposition is very important in order to obtain the good ferroelectricity of *c*-axis oriented BNN thin film.

2. EXPERIMENTAL

BNN thin films were deposited on (100)-oriented LSTO substrate by PLD method using BNN ceramic target. The single crystals of LSTO substrates, which were grown by the Czochralski method, were obtained from Earth Jewelry Co. Ltd. The BSNN ceramic target was prepared as follows. $BaCO_3$, $NaCO_3$ and Nb_2O_5 powders were mixed with cation molar ratio of Ba:Na:Nb=2:1:5 using a wet ball mill. The mixture was pressed into a disk shape at 4.9 kg/cm^2 and sintered for 6 h at 1350°C. The target disk was polished to 21.5 mm diameter and 5 mm thickness. The density of BNN target was approximately 98 % [15]. The target was examined using X-ray diffraction (XRD) with CuKα [15].

The PLD system was arranged in a symmetric configuration with a rotating substrate holder for

compositional uniformity. The base pressure was ordinaly 2×10^{-8} Torr, and substrate was inserted from a load lock chamber to maintain a low base pressure. A KrF excimer laser (λ=248 nm) was used for ablation of target. The laser power density and repetition frequency were 200 mJ/cm^2 and 5 Hz, respectively. The film thickness was approximately 400 nm. The top Pt electrodes with a diameter of 0.2 mm were deposited on the film surface through a metal shadow mask by rf-magnetron sputtering. The as-deposited BNN thin films were annealed at 700°C in an O_2 atmosphere for 1h in order to investigate the effect of post-annealing.

The structural properties of the BNN thin films were characterized by XRD. The surface morphologies were observed by AFM. The electrical properties were measured by using the ferroelectric property measurement system RT-6000HVS manufactured by Radiant Technologies. The polarization-voltage (*P-V*) hysteresis loops were measured using one-shot triangular waveforms with period of 50 ns.

3. RESULTS AND DISCUSSION

Figure 2 shows the XRD patterns as a function of T_{sub} for the BNN thin films. Po_2 was fixed at 7.5 mTorr. The (100) and (200) peaks of the LSTO substrates are observed at 2θ=22.8 ° and 46.5 °, respectively. The (002) and (004) peaks of the BNN thin films are observed at 2θ=22.2 ° and 45.3 °, respectively. The (350) peak is also observed at 2θ=29.5 °. The BNN thin films prepared at T_{sub}=650°C do not show the (002), (002) and (004) peaks, since the BNN thin films did not crystallize at 650°C. The BNN thin film at T_{sub}=750°C exhibits (350) peak as well as (002) and (004) peaks. Thus, the BNN thin films prepared at 700 °C exhibit a strong *c*-axis orientation.

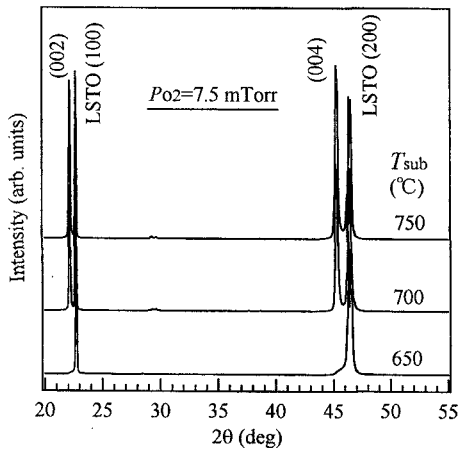

Fig. 2 XRD patterns as a function of Tsub in BNN thin films. Po2 is fixed at 7.5 mTorr.

Figure 3 shows the XRD patterns as a function of Po_2 for the BNN thin films. T_{sub} was fixed at 700°C. The *c*-axis peak of the BNN thin films is observed at all Po_2 values. The intensity of the (004) peak does not depend on Po_2 below 10 mTorr, though it decreases rapidly at Po_2>10 mTorr. The intensity of the (350) peak increases with Po_2. Therefore, the strong *c*-axis orientation of the BNN thin film is observed in the Po_2 region between 5 and 10 mTorr. The Po_2 of the strongly *c*-axis-oriented BNN thin film accords with that of the BNN thin film on a MgO substrate, as reported by Masuda and coworkers [9-11] and Xia *et al* [18]. The above result indicates that a low Po_2 below 10 mTorr is effective for the deposition of perfect BNN thin films. The BNN thin films deposited at Po_2>10 mTorr had a nonstoichiometric composition, although those deposited at Po_2<10 mTorr had a stocihiometric composition. Deposition rate does not change in this Po_2 region [13]. Therefore, the orientation of the BNN thin film is not related to deposition rate. This is considered to be due to the effects of impurities and stick molecules in the deposition chamber in the high-Po_2 region.

The above results indicate that the delicate control between T_{sub} and Po_2 during the deposition is important in obtaining strongly *c*-axis-oriented BNN thin film. Po_2 during the deposition of BNN thin films is closely related to T_{sub}, since the amount of oxygen vacancies in the thin film increases with temperature, as was previously clarified from the electrical resistivity of BNN thin films [11].

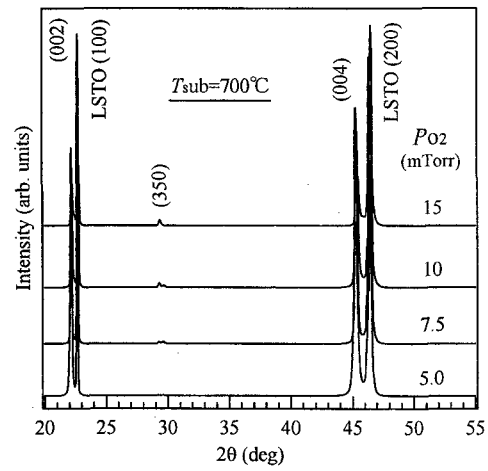

Fig. 3 XRD patterns as function of Po_2 for BNN thin films. T_{sub} is fixed at 700°C.

Figure 4 shows surface roughness and grain size as functions of Po_2 for the BNN thin films. T_{sub} was fixed at 700°C. Surface roughness increases with Po_2. Grain size does not change at Po_2<10 mTorr but increases at Po_2>10 mTorr. In particular, the grain size at Po_2=50 mTorr is equal to the film thickness and surface roughness. The poor surface roughness and large grain size at Po_2=15 mTorr might have originated from the three-dimensional islandlike crystal growth [19]. The particles ablated from the target migrate on the heated substrate and form crystal nuclei at step or kinds on the substrate due to the large energy at the interface of the BNN thin film and the substrate.

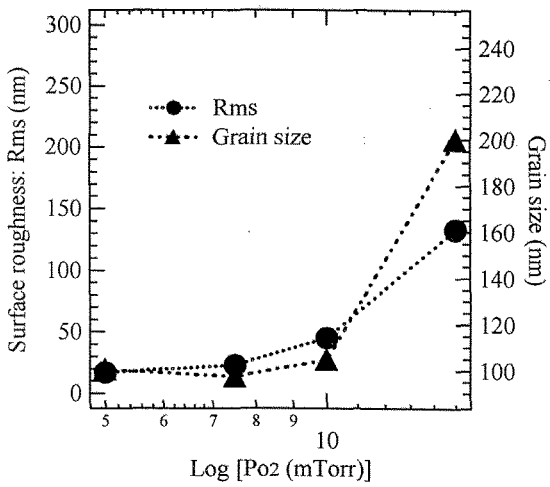

Fig. 4 Surface roughness (Rms) and grain size as functions of Po_2 for BNN thin films.

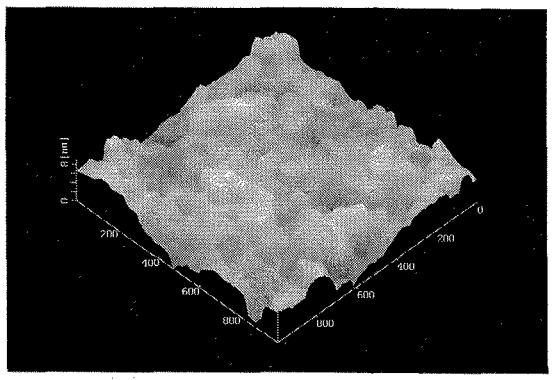

Fig. 5 AFM images of BNN thin films deposited at Po_2=7.5 mTorr. T_{sub} is fixed at 700°C.

Figure 5 shows the AFM image of the strongly *c*-axis-oriented BNN thin film prepared at T_{sub}=700 and Po_2=7.5 mTorr. The BNN thin film consisted of well-developed grains with a diameter of 100 nm. Its surface roughness was approximately 8 nm against a film thickness of 400 nm.

Figure 6 shows the hysteresis loops as a function of Po_2 for the BNN thin films. T_{sub} was fixed at 700°C. The BNN thin films at Po_2>15 mTorr did not exhibit ferroelectricity due to Na deficiency. The hysteresis loop of the BNN thin film is observed at Po_2=5.0, 7.5 and 10 mTorr. Although the BNN thin film at Po_2=10 mTorr is uniquely thin and has a low Ec, its Pr is very small. The BNN thin film at Po_2=7.5 mTorr shows good hysteresis loops. Then, P_r and E_c were $2P_r$=48.5 μC/cm^2 and $2E_c$=290 kV/cm, respectively. The leakage current was improved from ~10^{-3} A/cm^2 to ~10^{-6} A/cm^2 by the postannealing. The dielectric constant (ε_r) was approximately 180. These values are superior to those of the BNN thin films obtained by rf magnetron sputtering and the sol-gel method [9-12]. The good ferroelectricity of the strongly *c*-axis-oriented BNN thin film at Po_2=7.5 mTorr contributes to the small grain size and the smooth surface, as shown in Fig. 5.

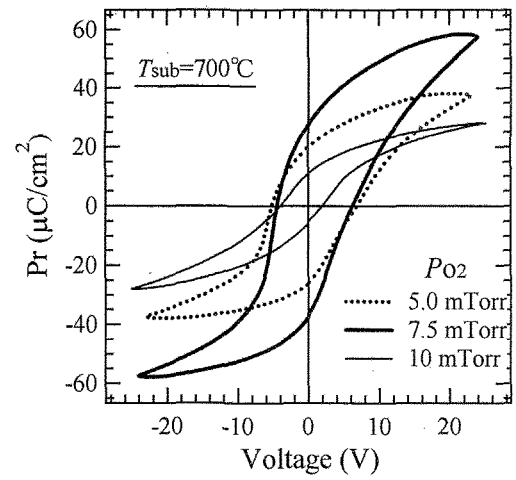

Fig. 6 *P-V* hysteresis loops as function of Po_2 for BNN thin films.

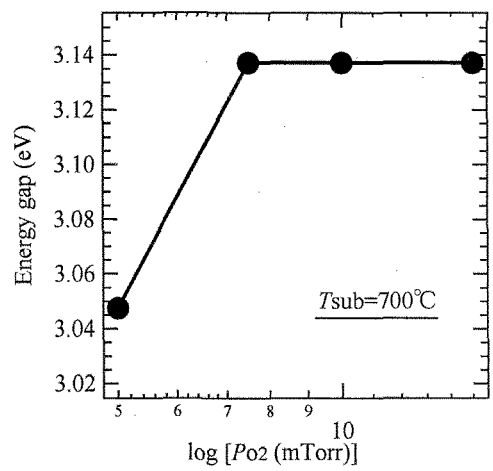

Fig. 7 Energy gap as function of Po_2 for BNN thin films.

Figure 7 shows the energy gap (E_g) as a function of Po_2 for the BNN thin films. T_{sub} was fixed at 700°C. The E_g of BNN thin film prepared at 5mTorr is smaller than that of BNN bulk crystal. This is considered to be due to oxygen vacancies.

In recent years, Fujihashi *et al.* studied the structural and optical properties of BNN thin films on Pt and quartz substrates prepared by the sol-gel method using $Ba(CH_3COO)_2$, $NaNO_3$, and Nb(O-n-Bu) [12]. The BNN thin film annealed at 800°C for 1 h exhibited a single phase. The BNN thin film had the leakage current effect due to the formation of pinholes at high postannealing temperatures. The band gap was approximately 2.7 eV, which is smaller than the band gap of the BNN bulk crystal [20]. The reason for this is considered to be the change in O 2*p* bandwidth or the existence of impurities in the BNN thin film. When the as-deposited BNN thin film was postannealed at 800°C, the BNN thin film formed oxygen vacancies and showed Na deficiency. On the other hand, we have already clarified that Na deficiency is induced at a postannealing temperature above 750°C and the volatility of Na in

BNN thin films is controlled at a postannealing temperature below 750°C. The postannealed BNN thin film prepared in this study has controlled Na deficiency. Thus, the band gap of the strongly *c*-axis-oriented BNN thin film is in good agreement with that of the BNN bulk crystal [20], as shown in Fig. 6.

4. CONCLUSION

We have studied the structural and ferroelectric properties of BNN thin films on LSTO substrates prepared by PLD. When Po_2 and T_{sub} were fixed at 7.5 mTorr and 700°C, respectively, the prepared BNN thin film exhibited strongly *c*-axis-orientation. This film consisted of well-developed grains and exhibited a good *P-V* hysteresis loop. Its P_r and E_c were $2P_r$=48.5 $\mu C/cm^2$ and $2E_c$=290 kV/cm, respectively. The band gap of this strongly *c*-axis-oriented BNN thin film was about 3.1 eV, which accords with that of the BNN single crystal.

ACKNOWLEDGEMENTS

We would like to thank Prof. Y. Masuda and Mr. M. Sogawa for their useful discussions. This work was partially supported by the Foundation for Materials Science and Technology of Japan (MST Foundation), and the Grant-In-Aid for Scientific Research from the Ministry of Education, Cultures, Sports, Science and Technology.

REFERENCES

[1] F. R. Nash, E. H. Turner, P. M. Bridenbaugh and J. M. Dziedzie: J. Appl. Phys. **42** (1972) 1.
[2] E. A. Giess, B. A. Scott, G. Burns, D. F. Okane and A. Segmuller: J. Am. Ceram. Soc. **52** (1969) 276.
[3] E. A. Giess, G. Berns, D. F. Okane and A. W. Smith: Appl. Phys. Lett. **11** (1967) 233.
[4] J. E. Geusic, H. J. Levinstein, S. Singh, R. G. Smith and L. G. Van Uitert: Appl. Phys. Lett. **12** (1968) 306.
[5] P. B. Jamieson, S. C. Abrahams and J. L. Bernstein: J. Chem. Phys. **48** (1968) 5048.
[6] S. H. Wemple and M. DiDomenico: J. Appl. Phys. **40** (1969) 735.
[7] A. Agostinelli, G. H. Braunstein and T. N. Blanton: Appl. Phys. Lett. **63** (1993) 123.
[8] L. S. Hung, J. A. Agostinelli and J. M. Mir: Appl. Phys. Lett. **62** (1993) 3071.
[9] Y. Masuda, H. Masumoto, A. Baba, T. Goto and T. Hirai: Jpn. J. Appl. Phys. **32** (1993) 4043.
[10] Y. Masuda, H. Masumoto, Y. Kidachi, A. Watadzul, A. Baba, T. Goto and T. Hirai: Jpn. J. Appl. Phys. **34** (1995) 5124.
[11] Y. Masuda, H. Masumoto, A. Baba, Y. Kidachi and T. Hirai: Ferroelectrics **195** (1997) 297.
[12] G. Fujihashi, A. Kakimi, S. Ando, S. Okamura, T. Tsuchiya and T. Tsukamoto: J. Ceram. Soc. Jpn. **105** (1997) 449.
[13] K. Ohnuki, T. Higuchi, M. Takayasu, M. Sogawa and T. Tsukamoto: Proc. Inter. Symp. Appl. Ferro. (ISAF) **XIII** (2002) 171.
[14] M. Sogawa, T. Higuchi, T. Kamei and T. Tsukamoto: Jpn. J. Appl. Phys. **42** (2003) 6990.
[15] T. Higuchi, M. Sogawa, T. Kamei and T. Tsukamoto: Trans. Mater. Res. Soc. Jpn. **29** (2004) 1117.
[16] T. Kamei, T. Higuchi, M. Sogawa, Y. Ebina, T. Hattori, Y. Masuda and T. Tsukamoto: Jpn. J. Appl. Phys. **43** (2004) 6617.
[17] Y. Tokura, Y. Taguchi, Y. Okada, Y. Fujishima, T. Arima, K. Kumagai and Y. Iye: Phys. Rev. Lett. **70** (1993) 2126.
[18] H. R. Xia, L. J. Hu, C. J. Wang, L. X. Li, S. B. Yue, X. L. Meng, L. Zhu, Z. H. Yang, and J. Y. Wang: J. Appl. Phys. **83** (1998) 2560.
[19] M. Nakano, H. Tabata, K. Tanaka, Y. Katayama and T. Kawai: Jpn. J. Appl. Phys. **36** (1997) L 1331.
[20] V. V. Voronov, Kuz'minov, S. Yu and I. G. Lukina: Sov. Phys. Solid State **18** (1976) 598.

(Received December 23, 2004; Accepted January 31, 2005)